International Journal of
Nanoscience and Nanotechnology

Research Article 2025, Volume 21, Issue 2

Enhancing the Ionic Conductivity of Corn Starch-Based Solid Polymer Electrolytes Utilizing Inorganic Fillers

Reffy Aldo Amanta[1], Sylvia Ayu Pradanawati[2], Yatim Lailun Ni'mah[3], Azzah Dyah Pramata[4], Lukman Noerochim[4], Nur Laila Hamidah[1*]

Received 12 October 2025
Accepted 25 March 2025

DOI: 10.22034/ijnn.2026.2043238.2581

International Journal of Nanoscience and Nanotechnology

Abstract

For safety reasons, solid polymer electrolytes (SPEs) have been developed as an alternative to liquid electrolyte. Nevertheless, the research advancement of all-solid-state energy storage is impeded by the ion transport between solid-solid interfaces. The incorporation of fillers into polymer matrices is a common approach to improve ion transport. The objective of this study is to enhance the ionic conductivity of corn starch-based SPE by incorporating zinc oxide (ZnO), vanadium oxide (V_2O_5), and cerium oxide (CeO_2) as inorganic fillers through the solution casting method. X-ray diffraction (XRD) indicated that the incorporation of 20 wt.% ZnO resulted in the highest amorphous state of 93%, thereby enhancing the ionic conductivity due to increased pathways for ion transfer. This finding was further supported by the analysis of the glass-transition temperature (T_g), recorded at 25.6°C via differential scanning calorimetry (DSC), thereby reinforcing the evidence for the amorphous state. The shift of the CH_2OH band from 1330 to 1321 cm^{-1} in Fourier transform infrared spectroscopy (FTIR) indicates the presence of the filler in the polymer structure. Moreover, the increased amorphous content leads to the formation of pores, as evidenced by scanning electron microscopy (SEM), which enhances the ionic conductivity of the solid polymer electrolyte (SPE). The ionic conductivity of the SPE containing 20 wt. % ZnO at ambient temperature is 3.021×10^{-3} S/cm, as measured by electrochemical impedance spectroscopy (EIS). This result is comparable to the ionic conductivity of liquid electrolytes ($10^{-4} - 10^{-2}$ S/cm), indicating possible applicability as a solid electrolyte.

Keywords: Amorphous state, Corn starch, Inorganic filler, Ionic conductivity, Solid polymer electrolyte

How to cite this article

Amanta RA, Pradanawati SA, Ni'mah YL, Pramata AD, Noerochim L, Hamidah NL. Enhancing the Ionic Conductivity of Corn Starch-Based Solid Polymer Electrolytes Utilizing Inorganic Fillers. Int. J. Nanosci. Nanotechnol., 2025;2: 67-75. DOI: 10.22034/ijnn.2026.2043238.2581

1. Introduction

Fossil fuels have long been the main source of energy to meet escalating global energy demands. Nonetheless, the use of fossil fuels has numerous negative impacts, including heightened pollution and global warming [1]. Recently, the need for efficient energy storage systems has grown due to finite fossil fuel resources and the global population growth. Consequently, society is transitioning to sustainable energy sources with higher energy and power density [2]. Recent advancements in energy storage systems include lithium-ion batteries (LIBs) and supercapacitors (SCs), both of which exhibit superior electrochemical characteristics, including high energy density and extended cycle life [2, 3].

Batteries often utilize liquid electrolytes; however, these present concerns such as higher flammability and leakage. In contrast to liquid electrolytes, Solid Polymer Electrolytes (SPEs) are being utilized and developed due to their advantages, including superior mechanical strength and chemical reaction neutrality, which mitigate side reactions with electrodes and hinder crystallization in batteries. Consequently, SPE is a promising discovery for the development of lithium batteries with a high level of safety, stability and energy density [4].

However, SPEs also still suffer from a significant weakness, namely, their very low ionic conductivity (10^{-11} - 10^{-9} S/cm) which is highly undesirable when compared with liquid electrolytes (10^{-4} - 10^{-1} S/cm) at room temperature [4, 5]. High ionic conductivity is desired because it allows electrons to move freely within the battery system, increasing the electric current and

[1] *Departement of Engineering Physics, Institut Teknologi Sepuluh Nopember, Kampus ITS Sukolilo, Surabaya 60111, Indonesia*

[2] *Department of Mechanical Engineering, Universitas Pertamina, Jalan Teuku Nyak Arief, Simprug Kebayoran Lama, Jakarta 12220, Indonesia*

[3] *Departement of Chemistry, Institut Teknologi Sepuluh Nopember, Kampus ITS Sukolilo, Surabaya 60111, Indonesia*

[4] *Departement of Material and Metallurgical Engineering, Institut Teknologi Sepuluh Nopember, Kampus ITS Sukolilo, Surabaya 60111, Indonesia*

** E-mail: nurlaila@its.ac.id*

thus the efficiency of electrochemical devices [6].

The use of synthetic polymers as a base for SPE is currently under development, but this raises environmental concerns because most of them are petroleum-derived and not readily biodegradable [7]. Many countries in the world are currently emphasizing energy consumption and the use of environmentally friendly materials to implement sustainable systems, so that biopolymer materials such as starch, polylactic acid, chitosan, etc. are being intensively developed to become materials that have the potential to replace the use of conventional plastics [8].

Starch-based biopolymers are abundant, cheap, easy to shape, environmentally friendly, and have the same molecular structure as petroleum-based plastics [9]. The researchers considered employing natural polymers or composites with natural polymers, such as starch, as SPE [10]. Starch is a semi-crystalline material from a combination of amylose with a long chain structure and amylopectin with a branched chain structure [11]. Amylose can recrystallize into a single helix, and amylopectin can recrystallize into a double helix through a process called retrogradation, which reconstructs the starch's crystalline structure. High levels of amylose are desirable, as the single helix structure facilitates easier electron passage than the double helix structure [8]. One starch source that contains a high level of amylose is corn starch which has an amylose concentration of 28% so it can be a candidate for use as a base in SPE. [12]. However, corn starch-based SPEs has low ionic conductivity at low temperatures (10^{-10} - 10^{-9} S/cm) and the degree of crystallinity was low as indicated by the many peaks in the XRD analysis [6, 11, 13]. One of many methods used to increase the ionic conductivity of SPE is by the addition of filler compounds. *Qin et al.* stated that the addition of fillers can increase the ionic conductivity value to reach 10^{-2} S/cm [14]. One type of filler currently being developed is an inorganic filler because it can reduce the rate of crystallization, resulting in a more amorphous structure and increases polymer chain mobility, which can enhance ion transport [4].

Feng et al. stated that the usage of 5 wt.% vanadium oxide (V_2O_5) in PVDF-based SPE shows poor crystallinity, very low glass-transition temperature (T_g), and high ionic conductivity, namely reaching 1.1 × 10^{-2} S/cm whereas using more than 20 wt.% could reduce ionic conductivity due to limited solubility [5]. *Ao et al.* used 8 wt.% cerium oxide (CeO_2) in the form of nanowires (NWs), which increased ionic conductivity with a value of 1.1× 10^{-3} S/cm. This happens because the NW filler seems to create a path for Li^+ ions to move more freely than using NP filler [15]. Based on research conducted by *Mokhtar et al.,* the use of 20 wt. % zinc oxide (ZnO) filler can increase ionic conductivity to 1.61×10^{-2} S/cm at room temperature, and reduce crystallinity [16]. Therefore, this research will focus on the effect of the type and concentration of inorganic fillers used to increase the ionic conductivity of corn starch-based SPE.

2. Experimental Procedure

2.1. Synthesis of Solid Polymer Electrolyte (SPE)

In this study, Corn starch $(C_6H_{10}O_5)_n$ was obtained from an online retailer (Maizenaku) with amylose content of 28%. Lanthanum nitrate ($La(NO_3)_3$) with 99.9% purity was obtained from Sigma-Aldrich. Inorganic filler - cerium oxide (CeO_2), vanadium pentoxide (V_2O_5), and zinc oxide (ZnO) – with 99.8% purity was obtained from Sigma-Aldrich.

SPE was synthesized using solution casting with 1.5 g corn starch, 25 mL water, 0.8 mL glycerol, and varying amounts (0%, 5%, 10%, 20%) of V_2O_5, CeO_2, or ZnO fillers. 0.5 g (25 wt.%) of $La(NO_3)_3$ was also added. SPE synthesis is initiated by diluting corn starch, lanthanum nitrate, and glycerol in distilled water with a magnetic stirrer. After that, fillers were added in corn starch solution until fully dispersed. The mixture was then placed in a water bath and stirred at 85°C for 1 hour to ensure homogeneity. The solution was then allowed to cool to room temperature to remove air bubbles. Finally, the mixture was poured into a petri dish and dried in an oven at 40°C until an SPE film formed.

2.2. Properties Measurement

The synthesized SPE samples were characterized using an X-ray diffractometer (XRD, PanAnalytical, Empyrean) to analyze the amorphous or crystalline nature of the SPE films films. X-ray diffraction measurements were performed over an angular range of 5°–90° using Cu Kα radiation (λ = 1.54056 Å) with a Ni filter, at an accelerating voltage of 40 kV and a current of 100 mA. Measurements were conducted over a 2θ range of 5°–80°, with a scanning speed of 0.5°/min and a step size of 0.05° at room temperature. These parameters allowed for the analysis of the Full Width at Half Maximum (FWHM) and the degree of crystallinity of the SPE (equation 1).

$$X_c = \frac{A_c}{A_c + A_a} \quad (1)$$

where X_c is the degree of crystallinity, A_c is the width of crystalline area and A_a is for the width of amorphous area.

FTIR characterization was performed using a Thermo Scientific Nicolet iS10 to identify ionic interactions between corn starch, $La(NO_3)_3$, and the filler in the wavenumber range of 4000 cm^{-1} to 400 cm^{-1}. SEM characterization was performed using an FEI Inspect S50 at magnifications of 2500×, 5000×, and 10,000× to observe the surface morphology of the sample. DSC was used to determine the glass-transition temperature (T_g) and melting temperature (T_m) of the SPE samples. The measurement was carried out using a Mettler Toledo system with a scan rate of 10°C/min over a temperature range of 25–150°C. EIS is characterized using CS potentiostat/galvanostat (electrochemical workstation) with a frequency range of 1 MHz – 1 Hz, test signal voltage of 10 mV, and using three electrodes (reference, counter, and working). The

SPE underwent Electrochemical Impedance Spectroscopy (EIS) test to determine its electrochemical performance. For EIS preparation, the sample thickness was measured using a digital screw micrometer, and the sample was then clamped between aluminum plates serving as electrodes, as illustrated by the equivalent circuit in Figure 1. The Nyquist plot data were fitted to an equivalent circuit to obtain the bulk resistance value (Rb), and the ionic conductivity of the SPE sample can be calculated using Equation 2.

$$\sigma = \frac{l}{A.R_b} \quad (2)$$

where σ is the ionic conductivity of the SPE (S/cm), l is the SPE thickness (cm), A is the surface area of the SPE (cm^2), and Rb is the bulk resistance of the SPE (Ω).

3. Result and Discussion

3.1. SPE synthesis result

SPE was synthesized using corn starch as the matrix. $La(NO_3)_3$ was used as the salt, and glycerol was incorporated as a plasticizer. CeO_2, V_2O_5, and ZnO were employed as fillers at varying weight percentages (wt.%). Specifically, each filler was added at 5 wt.%, 10 wt.%, and 20 wt.% for its respective variations. The synthesis utilized the solution casting method [17], and the resulting SPEs are depicted in Figure 2.

3.1. X-Ray Diffraction Analysis

XRD was used to identify the crystallization degree of SPEs samples. Figure 3 shows that pure corn starch (CS) is an A-type starch, characterized by peaks in the XRD data at diffraction angles of 15.2°, 17°, 18°, and 23° [18, 19]. In the SPE, glycerol was utilized as a plasticizer, which resulted in the crystal structure of the starch changing from A-type to B-type, with peaks at 16.8°, 19.8°, and 22.2° [18, 20]. Because of the shift in crystal structure from a monoclinic to a hexagonal pattern, which increases water absorption and hydrogen bonding in SPE, the CS+Gly variant is more amorphous than pure CS [19]. Corn starch peak intensity significantly decreased and the peak angle widened when $La(NO_3)_3$ salt was added [21].

Fillers help in the process of salt dissociation, which raises the value of ionic conductivity [22]. Additionally, as Figure 3 illustrates, the filler acts as a physical barrier that may prevent crystals from growing in maize starch, resulting in a decrease in peak intensity and a broadening of the peak angle, which to the point where distinguishing these peaks becomes challenging. However, each filler used significantly decreases peak. The Degree of Crystallinity was calculated using Equation 1, with the results summarized in Table 1.

Based on Table 1, the lowest degree of crystallization occurs at ZnO filler with a value of 7.23% having the maximum amorphous region with an amorphous state of 92.77%. This phenomenon may occur because the addition of fillers hinders the growth of crystal formation in corn starch, thereby increasing the amorphous region in the SPE [24]. Furthermore, a higher amorphous content generally leads to increased ionic conductivity, as it provides more pathways for ion transport [15].

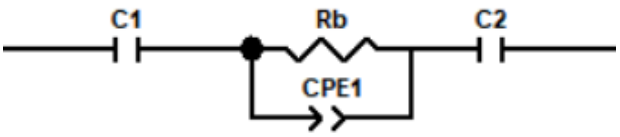

Figure 1. SPE equivalent circuit

3.2. Fourier Transform Infrared (FTIR) Spectroscopy Analysis

FTIR spectroscopy was used to investigate the interactions between the corn starch polymer, salt, and the inorganic filler used across all samples. Figure 4 shows the FTIR result of SPE.

The O-H functional group, which can bind water,

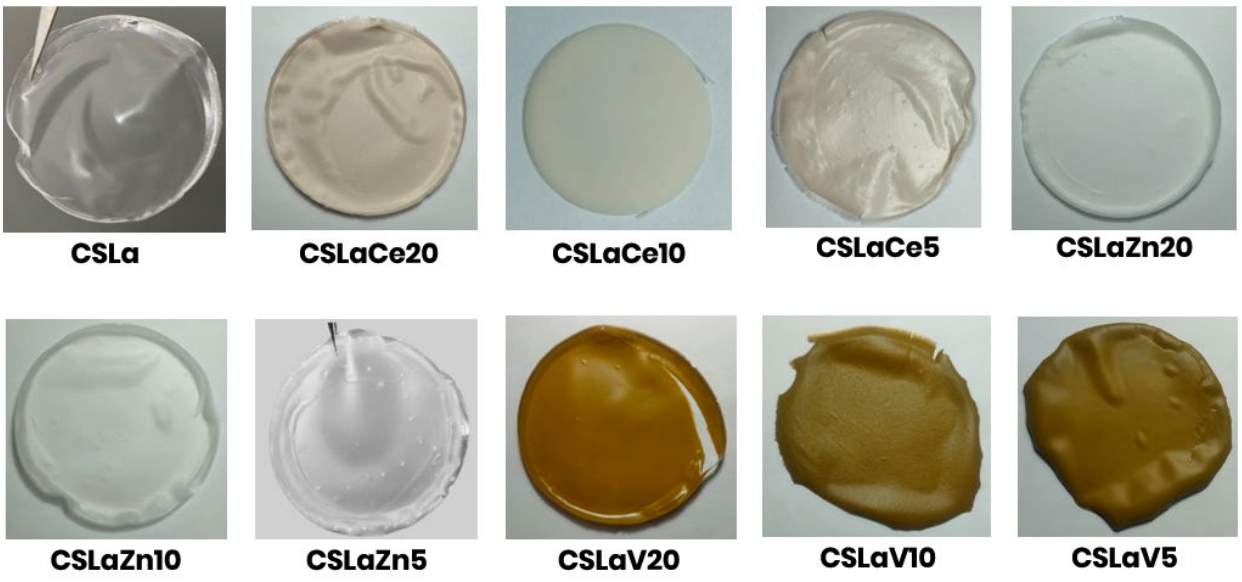

Figure 2. Corn starch based SPE synthesis results via solution casting method.

alter chemical structure, and cause salt dissociation in the 3458–3178 cm^{-1} wavenumber, is the first peak that could be observed [25, 26]. According to [18] adding glycerol may alter the binding structure by increasing the hydroxyl (O-H) group, which facilitates the process of salt dissociation and lowers the peak in CS+Gly. The addition of ($La(NO_3)_3$) salt resulted in the shifting and widening of the hydroxyl group peak, which moved from 3281 cm^{-1} to a lower wavenumber of 3261 cm^{-1} [16]. The use of fillers in nanoparticle form, which can attract water molecules, is thought to cause the observed shift of the O-H group to a lower wavenumber [27].

Vibrations at 1648 cm^{-1} are attributed to OH bending, a sign that water is present in the starch molecule [28]. In amorphous starch molecules, the addition of lanthanum salt strengthens the O-H bending and shifts it to a lower wavenumber of 1640 cm^{-1}, indicating a more stable hydrogen bond [16, 18, 29]. Moreover, CH_2-OH bending vibration at 1457, 1420, and 1330 cm^{-1} is linked to CH and CH_2 deformation [13, 30, 31]. The addition of filler lowers the intensity in CH_2 deformation which indicates a presence of filler [16]. Furthermore, it causes a shift in the CH_2-OH bending group and CH deformation to a lower wavenumber, indicating the location of complexation sites [32].

The C-O-H deformation and C-O-C stretching are indicated by peaks at 1021 and 991 cm^{-1}, respectively (Figure 4). The addition of salt, through the retrogradation process, breaks down amylopectin into amylose. This increases the amylose percentage, consequently making the SPE more amorphous [7, 8]. The breakdown of amylopectin into amylose also shows an increase in the C-O-H peak and a decrease in the C-O-C peak, which facilitates the complexation between the salt and polymer [21, 33]. Additionally, a peak at 860 cm^{-1} represents the C-O-C ring vibration of amorphous starch structures. [34]. The interaction mechanism of CS, La^{3+}, and filler proposed by FTIR analysis is shown in Figure 5.

Table 1. Degree of Crystallinity of corn starch based SPE.

Sampel	Amorphous State (%)	Crystallinity (%)
CS	48.56	51.44
CS + Gly	66.76	33.24
CSLa	84.32	15.68
CSLaCe	91.07	8.93
CSLaV	89.82	10.18
CSLaZn	92.77	7.23

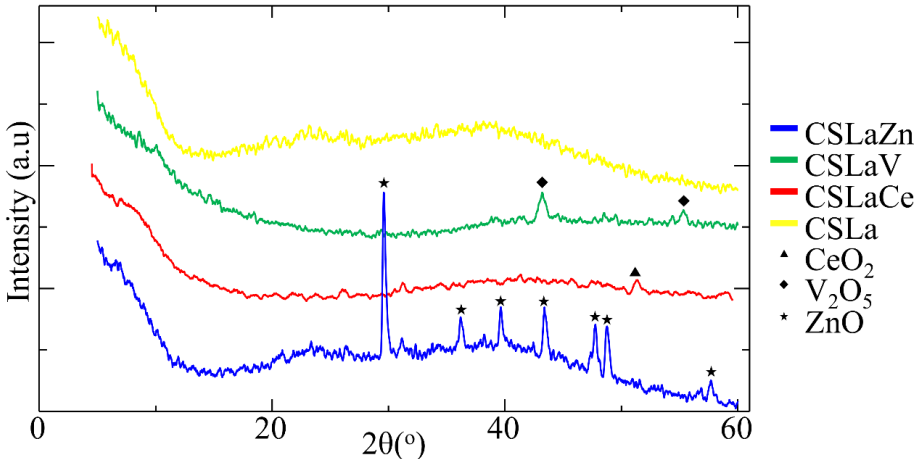

Figure 3. XRD pattern of corn starch based solid polymer electrolyte.

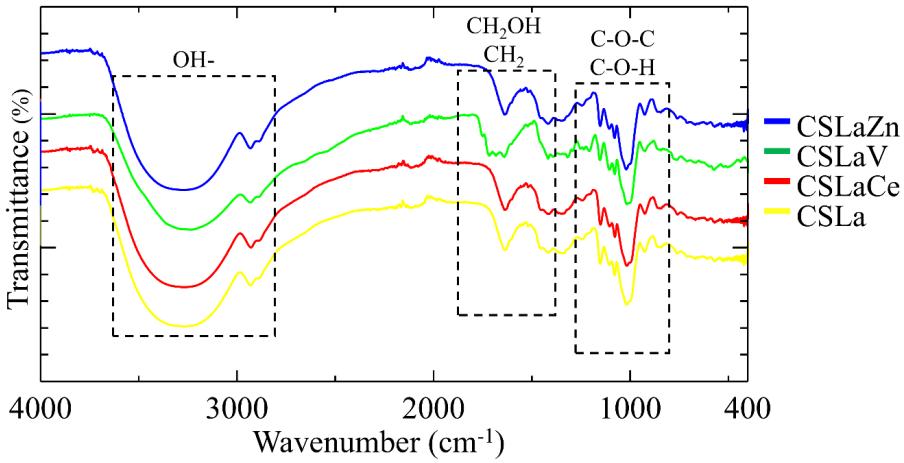

Figure 4. FTIR spectra for corn starch based solid polymer electrolyte.

3.3. Morphology Analysis

The Scanning Electron Microscope (SEM) has been used to verify the physical parameters of SPE samples through the analysis of the microscopic morphologies of the SPE particles. Figure 6 illustrates the morphology of SPE at a magnification of 5000×, showing a whitish mass recognized as corn starch (CS) which remains undissolved due to its poor solubility properties [35]. The addition of $La(NO_3)_3$ at 25 wt.% contributes to an increase in surface roughness, thereby enhancing the surface area [35]. Nonetheless, the incorporation of filler results in a gradual increase of surface defects and pore dispersion, with the CSLa:Zn sample exhibiting the most significant roughness [36, 37]. This structural deformation illustrates the dispersion of filler inside the polymer matrix, affecting surface homogeneity and promoting the formation of void networks [38].

The samples with filler exhibited a greater number of pores, corresponding to the overall condition of surface roughness. Materials characterized by diverse pore distributions typically exhibit this property [39]. The porosity ranged from 0.265% in CSLa, 1.095% in CSLaCe, 6.235% in CSLSV, to 6.937% in CSLaZn, with the observed enhancement indicating significant modifications in surface morphology, demonstrating the interaction between the polymer matrix and the filler [36].

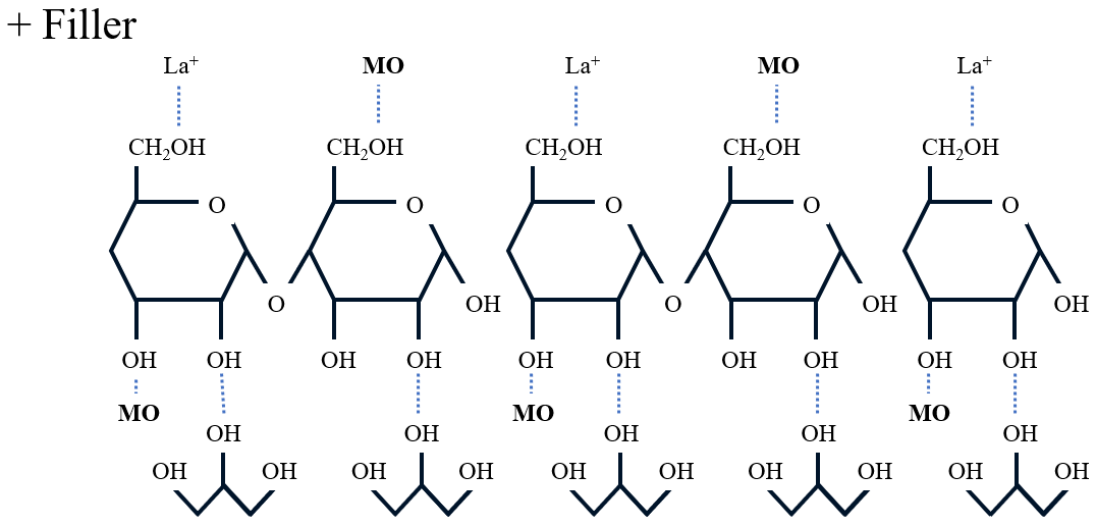

Figure 5. Proposed mechanism of corn starch molecule inhibiting inorganic filler.

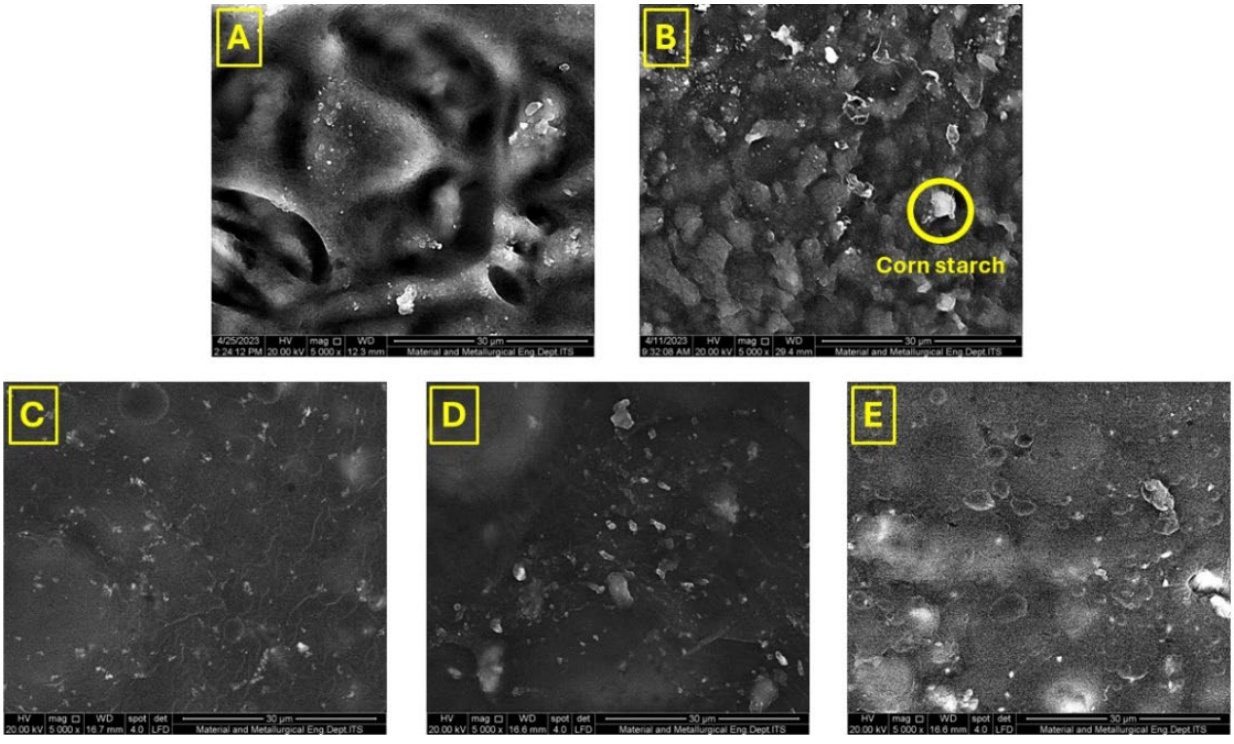

Figure 6. Surface morphology for (A) CS + Gly (B) CSLa (C) CSCe (D) CSV and (E) CSZn from SEM.

3.4. Thermal Stability Analysis

Solid Polymer Electrolyte (SPE) membrane thermal characteristics are examined using DSC and the results are shown in Figure 7. According to Figure 7A, the SPE membrane's melting temperature (T_m) is represented as an endothermic form peak on the DSC curve [40]. The CS+Gly variation's DSC curve demonstrates a large, shallow endothermic peak that denotes a highly crystalline structure [8]. A stronger (deeper) endothermic peak and a lower T_m of the SPE membrane could result from the addition of salt, such as lanthanum nitrate, as in the CSLa variation. This suggests a more amorphous and less rigid structure, which has been confirmed by XRD analysis [8, 41]. Because corn starch is in a lower crystalline condition following the addition of filler, the shifting of T_m may be much smaller [15].

The derivative curve of the DSC result, within the 25–35°C range, is displayed in Figure 7B to calculate the glass-transition (T_g) value of SPE. The glass-transition temperature (T_g) of the SPE membrane was calculated using a derivation approach based on the Heat Flow curve. *Apostolidis et al.* state that the T_g of the SPE membrane is indicated by the first peak on the first derivative heat flow curve corresponds to the highest (deepest) endothermic energy [42]. The addition of salt may reduce the T_g of the SPE membrane, as revealed by the first derivative heat flow curve in Figure 7, which reveals that CS-Gy and CSLa, have T_g of 26.3°C and 25.9°C, respectively [8, 41]. Additionally, filler helps to further reduce the T_g value [5]. Lower T_g values are preferred because they may indicate polymer mobility and are anticipated to increase ionic conductivity. This is the case with the CSLaCe, CSLaV, and CSLaZn variations, which have lower T_g values of 25.6°C, 26°C, and 25.6°C, respectively [43, 44].

3.5. Electrochemical Performance Analysis

Electrochemical impedance spectroscopy (EIS) was utilized to determine the ionic conductivity of the SPE film. The results of the measurement were then plotted on a graph, with Z' (Ohm) serving as the x-axis and Z'' (Ohm) serving as the y-axis, respectively. The results of the EIS test are depicted in Figure 8A, and Figure 1 depicts the equivalent circuit of SPE that is sandwiched between two electrodes. At low frequencies along the real Z axis, these data illustrate how the presence of filler can cause a change in the ionic conductivity value where depressed semicircle was shown for all membranes. The high-frequency semicircle reflects the dielectric behavior of

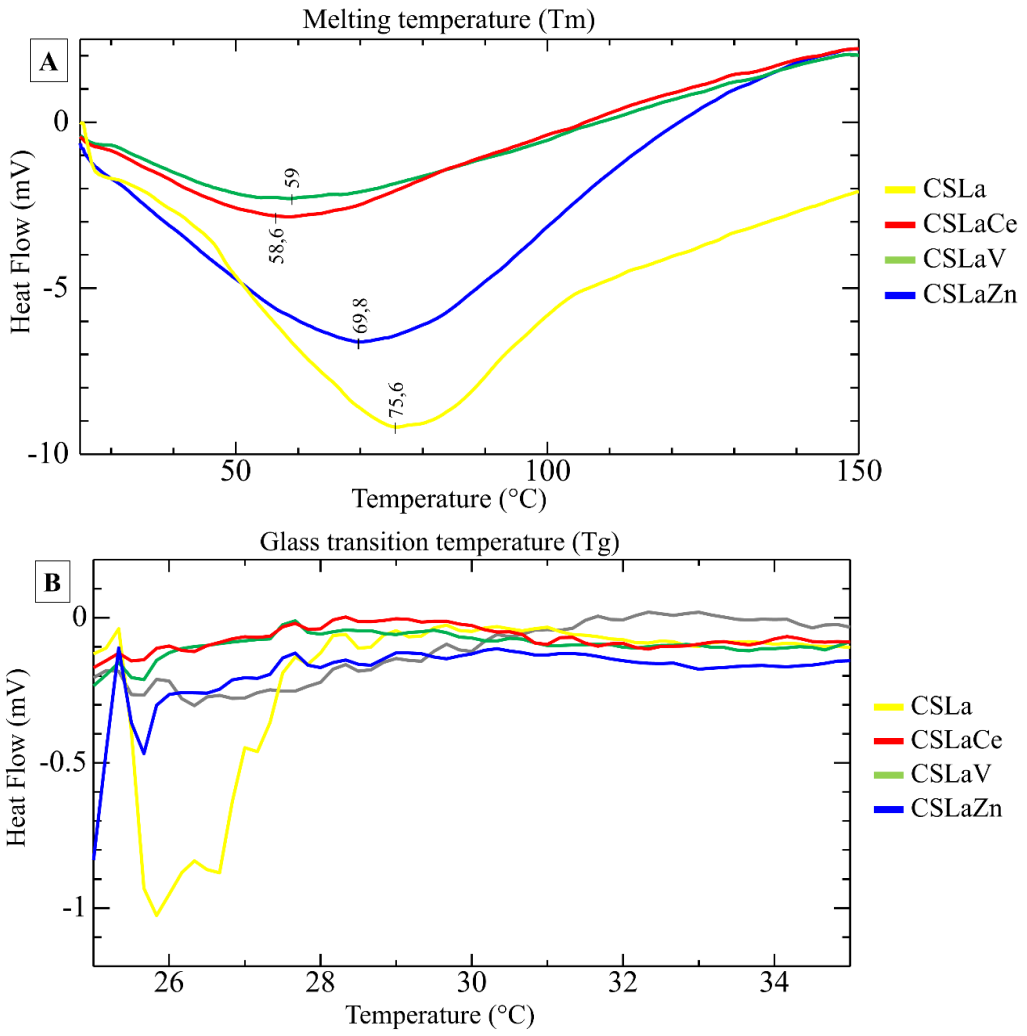

Figure 7. (A) DSC heating curve of corn starch based solid polymer electrolyte and (B) First derivative of DSC heating curve

Table 2. Ionic conductivity values of corn starch based SPE.

Sample	Rb (Ω)	A (cm^2)	l (cm)	σ (S/cm)	Percentage Change
CSLa	143	3.14	0.032	7.127×10^{-5}	-
CSLaCe5	83.28	3.14	0.055	2.103×10^{-4}	195.08%
CSLaCe10	79.48	3.14	0.055	2.204×10^{-4}	209.25%
CSLaCe20	40.84	3.14	0.055	4.289×10^{-4}	501.79%
CSLaV5	20.81	3.14	0.055	8.417×10^{-4}	1081.01%
CSLaV10	387.16	3.14	0.042	3.455×10^{-5}	-51.52%
CSLaV20	2193	3.14	0.062	9.004×10^{-6}	-87.36%
CSLaZn5	112.05	3.14	0.041	1.165×10^{-4}	63.46%
CSLaZn10	60.66	3.14	0.043	2.258×10^{-4}	216.82%
CSLaZn20	4.85	3.14	0.046	3.021×10^{-3}	4138.81%

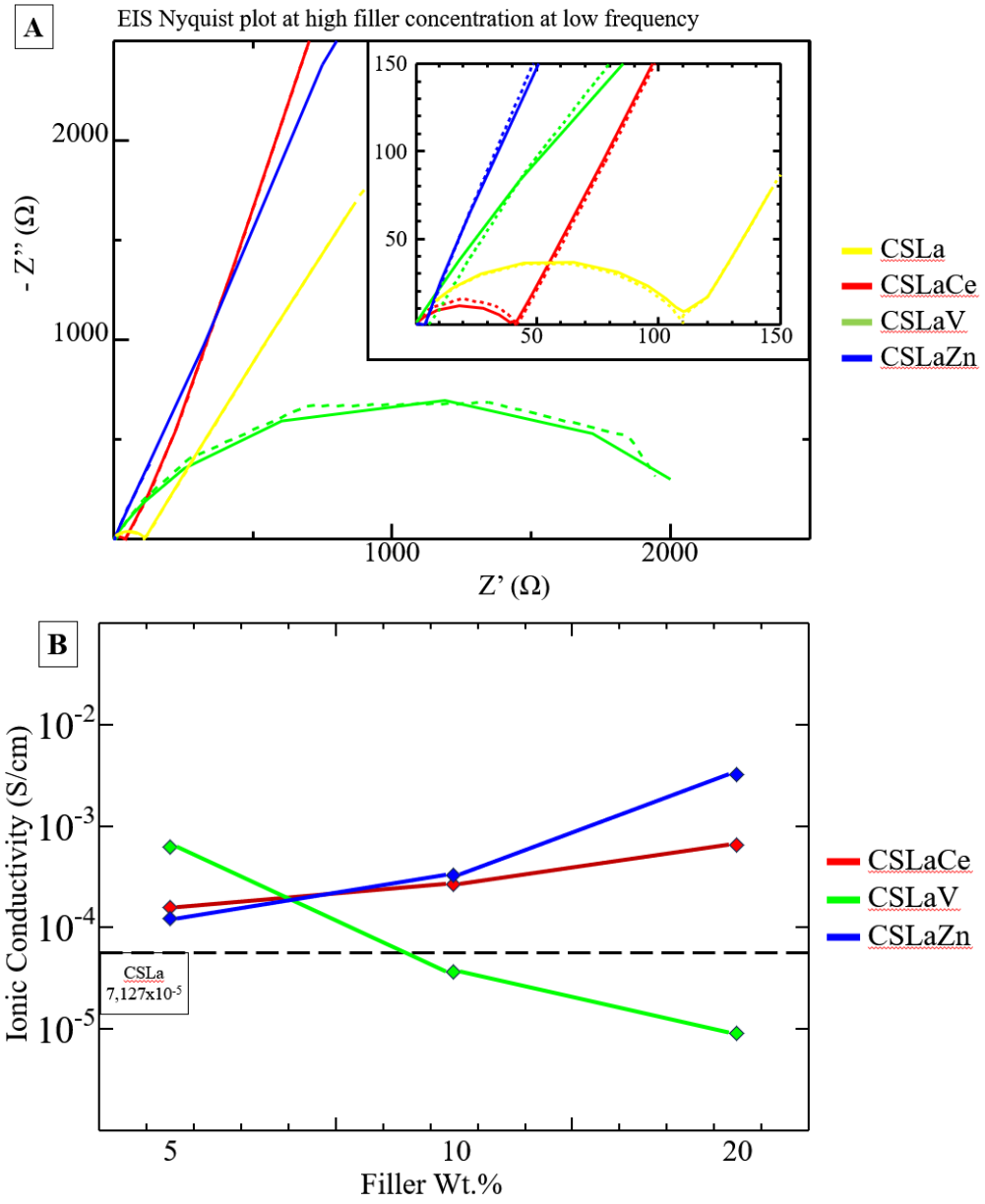

Figure 8. (A) Nyquist plot of corn starch based solid polymer electrolyte and (B) Ionic conductivity trend.

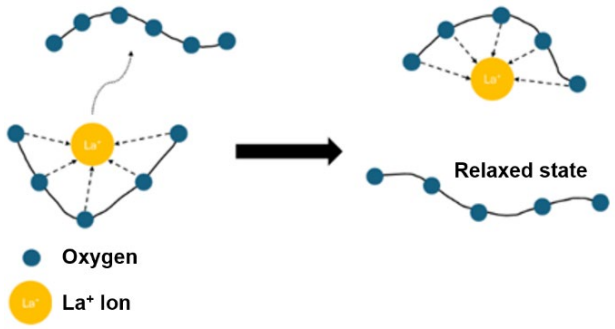

Figure 9. Proposed segmental motion mechanism in corn starch-based solid polymer electrolyte.

the SPE and can be modeled using parallel capacitive and resistive elements. The capacitive response is represented on the Z'' (imaginary) axis, whereas the resistive response appears on the Z' (real) axis [45]. The point between depressed semicircle and continuous slope (polarized state) was used to determine the bulk resistance (Rb) of SPE [46]. Therefore, the faster the SPE transitions into the polarized state, the better, because it indicates low bulk resistance and thus higher ionic conductivity [45]. Considering the results of the EIS plot, Equation 1 can be utilized to determine the ionic conductivity value of the SPE sample.

Based on previous research, pure corn starch has an ionic conductivity of10^{-10} S/cm [6]. Adding filler could increase the ionic conductivity even further since filler has a role in disrupting the crystalline growth of the SPE sample and making a pathway for a fast ion transport [15]. Thus, the highest conductivity from SPE is 3.021×10^{-3} S/cm with the addition of 20 wt.% ZnO. However, the addition of V_2O_5 results in a decrease in ionic conductivity value which is caused by a blocking effect in which filler restricts polymer chain mobility thus increasing the resistance [47].

The value of ionic conductivity in SPE is related to segmental motion. Segmental motion is a phenomenon involving ion hopping mechanism due to strain and relaxation movements in polymer chains as illustrated in Figure 9 [48]. An increase in the amorphous region improves the ionic conductivity which can promote cation intermolecular coordination, resulting in cations moving more easily [48, 49].

4. Conclusion

This work revealed that the incorporation of ZnO, CeO_2, and V_2O_5 as inorganic fillers into corn starch-based solid polymer electrolytes led to an enhancement in the amorphous state, as indicated by the characterization results. The amorphous structure of the polymer was confirmed by XRD results. The rise in the amorphous state resulted from the interaction between the polymer and salt, characterized by a reduction in C-O-C groups and a corresponding increase in C-O-H groups, which enhances hydrogen bonding among the polymer, salt, and filler, as indicated by FTIR analysis. Additionally, the SEM results indicated a transformation in the morphology of the SPE, resulting in an uneven grain pattern, the presence of pores, and an increase in surface roughness following the incorporation of filler. In addition, the amorphous nature of the SPE is corroborated by differential scanning calorimetry (DSC) analysis, which indicates that the filler can lower both the melting temperature (T_m) and the glass-transition temperature (T_g). The amorphous structure of the SPE is anticipated to exhibit enhanced ionic conductivity. Moreover, at a filler content of 20 wt.%, the maximum ionic conductivity of SPE with ZnO, CeO_2, and V_2O_5 were recorded for 3.02×10^{-3} S/cm, 4.29×10^{-4} S/cm, and 9.00×10^{-6} S/cm, respectively. V_2O_5 exhibited the lowest conductivity at elevated concentrations due to a blocking effect that initiates agglomeration reactions, thereby increasing resistance.

Acknowledgement

This research was financially supported by Institut Teknologi Sepuluh Nopember under the contract no: 1620/PKS/ITS/2024. The authors would like to thank the research assistants, Mr E. G. Izzul Haq, Ms M. R. Maulida, and Ms I. Z. Novia for their invaluable help in data collection and manuscript revision.

Conflict of interest

The authors declare that they have no conflict of interest.

References

1. Lasrado D, Ahankari S, Kar K. Review on recent advances in polymer nanocomposites for energy storage applications. J Appl Polym Sci. 2020;137(1):1-12. https://doi.org/10.1002/app.48959
2. Tafete GA, Abera MK, Thothadri G. Review on nanocellulose-based polymer nanocomposites for energy storage applications. J Energy Storage. 2022;48:103938. https://doi.org/10.1016/j.est.2021.103938
3. Sasikumar M, Krishna RH, Raja M, Therese HA, Balakrishnan NTM, Raghavan P, et al. A review on polymer electrolytes for lithium-ion batteries. J Alloys Compd. 2021;882:160709. https://doi.org/10.1016/j.jallcom.2021.160709
4. Yang X, Liu J, Pei N, Chen Z, Li R, Fu L, et al. The Critical Role of Fillers in Composite Polymer Electrolytes for Lithium Battery. Singapore: Springer Nature; 2023. https://doi.org/10.1007/s40820-023-01051-3
5. Feng T, Hu Y, Xu L, Huang J, Hu S, Zhang L, et al. Recent advances in solid-state polymer electrolytes for lithium batteries. Mater Today Energy. 2022;28:101062. https://doi.org/10.1016/j.mtener.2022.101062
6. Anandha JM, Vanitha D, Sundaramahalingam K, Nallamuthu N. Development and characterization of PEO-based solid polymer electrolytes for energy storage applications. Ionics. 2022;28:1809-1820. https://doi.org/10.1007/s11581-022-04446-1
7. Teoh KH, Lim CS, Ramesh S. Electrical and electrochemical properties of polymer electrolytes. Measurement. 2014;48:87-95. https://doi.org/10.1016/j.measurement.2013.10.040
8. Lai DS, Osman AF, Adnan SA, Ibrahim I, Salimi MNA, Alrashdi AA. Polymer electrolytes for energy storage devices: a review. Polymers (Basel). 2022;14(15):3125. https://doi.org/10.3390/polym14132567
9. Jiang T, Duan Q, Zhu J, Liu H, Yu L. Recent advances in polymer electrolytes for lithium batteries. Adv Ind Eng Polym Res.

2020;3(1):8-18.
10. Hadad S, Hamrahjoo M, Dehghani E, Salami-Kalajahi M, Eliseeva SN, Moghaddam AR, et al. Polymer electrolytes for lithium-ion batteries: a review. Appl Energy. 2022;324:119767. https://doi.org/10.1016/j.apenergy.2022.119767
11. Nandhinilakshmi M, Vanitha D, Nallamuthu N, Anandha JM, Sundaramahalingam K. Effect of filler on the electrochemical properties of polymer electrolytes. Polym Bull. 2023;80:3793-3808. https://doi.org/10.1007/s00289-022-04230-1
12. Surendren A, Mohanty AK, Liu Q, Misra M. Green polymer electrolytes for energy storage applications. Green Chem. 2022;24(22):8606-8630. https://doi.org/10.1039/D2GC02169B
13. Jothi MA, Vanitha D, Sundaramahalingam K, Nallamuthu N. Nanofiller-based polymer electrolytes for energy storage. Int J Hydrogen Energy. 2022;47(63):28763-28776. https://doi.org/10.1016/j.ijhydene.2022.06.192
14. Qin H, Fu K, Zhang Y, Ye Y, Song M, Kuang Y, et al. Composite polymer electrolytes for high-performance lithium batteries. Energy Storage Mater. 2020;28:293-302. https://doi.org/10.1016/j.ensm.2020.03.019
15. Ao X, Wang X, Tan J, Zhang S, Su C, Dong L, et al. Recent progress in polymer electrolytes for lithium batteries. Nano Energy. 2021;79:105475. https://doi.org/10.1016/j.nanoen.2020.105475
16. Mokhtar M, Majlan EH, Ahmad A, Tasirin SM, Daud WRW. Polymer electrolytes for electrochemical energy storage. J Electrochem Soc. 2018;165(11):A2483-A2495. https://doi.org/10.1149/2.0381811jes
17. Awang FF, Hassan MF, Kamarudin KH. Review on polymer electrolytes for energy storage applications. Ionics. 2022;28:1249-1262. https://doi.org/10.1007/s11581-022-04444-3
18. Xu X, Wang B, Gao W, Sui J, Wang J, Cui B. Biopolymer-based electrolytes for energy storage. Front Nutr. 2023;10:1-12. https://doi.org/10.3389/fnut.2023.1335812
19. Wang B, Xu X, Fang Y, Yan S, Cui B, Abd El-Aty AM. Natural polymer-based electrolytes for sustainable energy storage. Front Nutr. 2022;9:1-10. https://doi.org/10.3389/fnut.2022.882682
20. Hazrol MD, Sapuan SM, Zainudin ES, Zuhri MYM, Wahab NIA. Biopolymer-based electrolytes for energy applications. Polymers (Basel). 2021;13(18):3160. https://doi.org/10.3390/polym13020242
21. Nithya Priya C, Muthuvinayagam M, Vahini M. Conductivity studies of polymer electrolytes. J Mater Sci. 2023;58:773-788. https://doi.org/10.1007/s10853-022-08098-4
22. Banitaba SN, Semnani D, Heydari-Soureshjani E, Rezaei B, Ensafi AA. Polymer nanocomposite electrolytes for energy storage. Mater Res Express. 2019;6(12):125345. https://doi.org/10.1088/2053-1591/ab25cd
23. Wu Y, Zhang Y, Liu Y, Feng J. Recent progress in polymer electrolytes for lithium batteries. Energy Technol. 2021;9(7):1-15.
24. Yang H, Wu N. Ionic conductivity and ion transport mechanisms of solid-state lithium-ion battery electrolytes: a review. J Power Sources. 2022;546:231986. https://doi.org/10.1002/ese3.1163
25. Abdalrahman AA, Aziz SB, Karim WO. Structural and electrical properties of polymer electrolytes. Results Phys. 2022;36:105439. https://doi.org/10.1016/j.rinp.2022.105439
26. Abdulwahid RT, Aziz SB, Kadir MFZ. Characterization of solid polymer electrolytes. J Phys Chem Solids. 2022;167:110774. https://doi.org/10.1016/j.jpcs.2022.110774
27. Naseem T, Durrani T. Polymer electrolytes for energy storage: a review. Environ Chem Ecotoxicol. 2021;3:59-68. https://doi.org/10.1016/j.enceco.2020.12.001
28. Seki T, Chiang KY, Yu CC, Yu X, Okuno M, Hunger J, et al. Ion transport mechanisms in polymer electrolytes. J Phys Chem Lett. 2020;11(20):8459-8465. https://doi.org/10.1021/acs.jpclett.0c01259
29. Li Z, Li X, Jiang Y, Ding Q, Han W. Characterization of polymer electrolytes for energy storage. Polym Test. 2021;104:107380. https://doi.org/10.1016/j.polymertesting.2021.107380
30. Dankar I, Haddarah A, Omar FEL, Pujolà M, Sepulcre F. Biopolymer-based electrolytes for sustainable applications. Food Chem. 2018;260:7-15. https://doi.org/10.1016/j.foodchem.2018.03.138
31. Gao L, Zhu T, He F, Ou Z, Xu J, Ren L. Polymer electrolytes for energy storage applications. Coatings. 2021;11(8):890. https://doi.org/10.3390/coatings11080890
32. Ahmed HT, Abdullah OG. Structural and electrical properties of polymer electrolytes. Results Phys. 2020;16:102913. https://doi.org/10.1016/j.rinp.2019.102861
33. Sikora M, Krystyjan M, Dobosz A, Tomasik P, Walkowiak K, Masewicz Ł, et al. Biopolymer electrolytes for energy storage. Polymers (Basel). 2019;11(11):1761. https://doi.org/10.3390/polym11111764
34. Basilio-Cortés UA, González-Cruz L, Velazquez G, Teniente-Martínez G, Gómez-Aldapa CA, Castro-Rosas J, et al. Polymer electrolytes from natural sources. Polymers (Basel). 2019;11(7):1126. https://doi.org/10.3390/polym11020333
35. Hu G, Lan X, Peng B, Liao J, Xiong Y. Biopolymer-based electrolytes for high-performance energy storage. Int J Biol Macromol. 2024;260:129476. https://doi.org/10.1016/j.ijbiomac.2024.129476
36. Huy VPH, So S, Hur J. Inorganic fillers in composite gel polymer electrolytes for high-performance lithium and non-lithium polymer batteries. Polymers (Basel). 2021;13(22):4021.
37. Sabrina Q, Sohib A, Lestariningsih T, Ratri CR. The effect of (TiO2 and SiO2) nano-filler on solid polymer electrolyte based LiBOB. J Phys Conf Ser. 2019;1171(1):012034. https://doi.org/10.1088/1742-6596/1191/1/012028
38. Bashirpour-Bonab H. Polymer electrolytes for energy storage devices. Int J Energy Res. 2022;46(13):1-20. https://doi.org/10.1002/er.8278
39. Awang FF, Hassan MF, Kamarudin KH. Review on polymer electrolytes for electrochemical devices. Acta Polytech. 2021;61(6):497-509. https://doi.org/10.14311/AP.2021.61.0497
40. Al-Gunaid MQA, T.E S, H.M G, Al-Ostoot FH, Basavarajaiah S. Nanofiller-based polymer electrolytes. Polym Plast Technol Mater. 2020;59(2):215-230. https://doi.org/10.1080/25740881.2019.1634729
41. Mustapa SR, Aung MM, Rayung M. Biopolymer-based electrolytes for energy applications. Polymers (Basel). 2021;13(20):3500. https://doi.org/10.3390/polym13010132
42. Apostolidis P, Elwardany M, Porot L, Vansteenkiste S, Chailleux E. Polymer-based materials for energy storage. Mater Struct. 2021;54(6):1-15. https://doi.org/10.1617/s11527-021-01726-6
43. Jia W, Li Z, Wu Z, Wang L, Wu B, Wang Y, et al. Composite polymer electrolytes for high-performance lithium batteries. Solid State Ionics. 2018;315:7-13. https://doi.org/10.1016/j.ssi.2017.11.026
44. Yao P, Yu H, Ding Z, Liu Y, Lu J, Lavorgna M, et al. Polymer electrolytes for energy storage applications. Front Chem. 2019;7:1-12. https://doi.org/10.3389/fchem.2019.00522
45. Debye P. Polar molecules and their applications. J Soc Chem Ind. 1929;48(41):1036-1041.
46. Abdul Halim SI, Chan CH, Apotheker J. Polymer electrolytes: a review. Chem Teach Int. 2021;3(2):117-126. https://doi.org/10.1515/cti-2020-0018
47. Dissanayake MAKL, Jayathilaka PARD, Bokalawala RSP, Albinsson I, Mellander BE. Polymer electrolytes for energy storage. J Power Sources. 2003;119-121:409-413. https://doi.org/10.1016/S0378-7753(03)00262-3
48. Dennis JO, Shukur MF, Aldaghri OA, Ibnaouf KH, Adam AA, Usman F, et al. Polymer electrolytes for electrochemical energy storage. Molecules. 2023;28(7):3125. https://doi.org/10.3390/molecules28041781
49. Ahmed MB, Nofal MM, Aziz SB, Al-Saeedi SI, Brza MA, Dannoun EMA, et al. Structural and electrochemical properties of polymer electrolytes. Arab J Chem. 2022;15(12):104196. https://doi.org/10.1016/j.arabjc.2022.104196